

# The Simulation of the Dynamic Processes at the Thermal Spraying of the Cr<sub>3</sub>C<sub>2</sub>-NiCr Powder Particles with High-Speed Flame

Doina Petrescu\*, Niculae Napoleon Antonescu\*, Juan Alberto Calero\*\*

\* Universitatea Petrol-Gaze din Ploiești, Bd. București 39, Ploiești, România  
e-mail: [dpetrescu@upg-ploiesti.ro](mailto:dpetrescu@upg-ploiesti.ro)

\*\* Universitat de Barcelona, 08028 Barcelona, Espagne

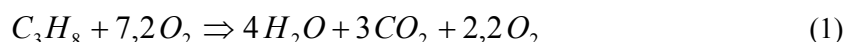
## Abstract

*In the paper there are presented the experimental research results made for the study of the mechanic and thermal behavior of the particle from the dynamic processes at thermal spraying with high – speed flame whose theoretical model was proposed in the paper [11]. The experimental tests were made in the Thermal Design Center Laboratories of the University of Barcelona.*

**Key words:** *thermal spraying, optimal parameters.*

## The Mathematical Simulation

The thermal problem and the mechanical one have solution with the help of the algorithms described in [1,2,11]. For the mathematical simulation will be considered the following reaction that takes place in the pistol combustion chamber:



The thermal spraying is made on a sub-layer of stanley tip 34Cr<sub>4</sub>Mo from different distances of spraying, thus 200mm, 300mm, 400mm [5,6,9,10].

The combustion products properties (viscosity, density, specific heat, thermal conductivity) used for determining the fluid parameters are obtained as average values.

There were calculated the fluid speed and the temperature following the points established in the paper [11].

**Tabel 1.** Powder properties

Properties	Ni	Cr	Cr <sub>3</sub> C <sub>2</sub>	Cr <sub>2</sub> O <sub>3</sub>
Density, kgm <sup>-3</sup>	8 900	7 190	6 600	5 210
Specific heat, Jkg <sup>-1</sup> K <sup>-1</sup>	471	460	300	880
Thermal conductivity, Wm <sup>-1</sup> K <sup>-1</sup>	83	67	95	22
Thermal diffusivity, 10 <sup>-5</sup> m <sup>2</sup> s <sup>-1</sup>	1,98	2,03	4,80	0,48
Latent fusion heat, 10 <sup>6</sup> Jkg <sup>-1</sup>	0,3	0,27	-	-

The spherical particles have diameter between 10μm and 60μm. The properties of the studied powder that takes part in the simulation are presented in the table (1). It is considered that the

presence of the carbon in the Ni-Cr metal stage does not decisively influence the thermal and physical properties so its influence is negligible.

For the basic variant of the calculus system there were used the following parameters: the particle ray  $d_p = 40\mu\text{m}$ ; the initial temperature of the particle  $T_{p0} = 1350^\circ\text{C}$ ; the equivalency relation  $R = 1,44$ ; the correlation factors  $b_1 = 0,84$ ,  $b_2 = 440$ ,  $b_3 = 0,03$ ; the initial speed of the particle  $v_{p0} = 305\text{m/s}$ ; the initial volumetric fraction of chrome carbide  $\varepsilon_0 = 0,3$ ; the initial volumetric fraction of chrome oxide  $\delta_0 = 0,005$ ; the final volumetric fraction of chrome oxide  $\delta = 0,05$ ; the propane discharge  $Q_{prr} = 60\text{ l/min}$ ; the oxygen discharge  $Q_{O_2} = 440\text{ l/min}$ ; the transporting gas discharge (azote)  $Q_{N_2} = 20\text{ l/min}$ ; the pistol length  $L = 0,1\text{ m}$ .

The thermal problem and the mechanical one have a solution with the help of the mathematical algorithms [11].

## Results and Commentaries

**The fluid's parameters.** The calculated values of the fluid speed, the temperature and the pressure in the critical points for the projection system with high-speed flame are presented in the table (2) [11].

**Tabel 2.** Fluids parameters in the critical points

Fluids parameters	Point 1	Point 2	Point 3
Speed, $\text{ms}^{-1}$	312	305	550
Temperature, $^\circ\text{C}$	2 771	2 600	2 165
Pressure, bar	3,37	2,50	1,0

The fluid speeds and temperatures, in relation with the projection distance are calculated by interpolation. The calculus' results as the particle's speed in relation with the spraying distance, spreading time and particle's diameter are presented in figure (1) and in figure (5).

**The mechanical behavior of the particle. Comparison with the experimentally obtained results.** In the projection with high-speed flame process, the particles speed from the spraying jet  $v_p$  is maximal in the point 3 [11]. (fig. 1).

The particles speed from the spraying jet decreases once with the increase of the particles' diameter  $d_p$ .

When the  $d_p$  diameter increases, the maximum speed  $v_{p,max}$  corresponding to the foreseen diameter will decrease and will go to the layer. That is why the particle with the highest diameter  $d_p$  varies the most uniformly with the speed along the projection distance.

The  $v_{p,max}$  value when it increases, leads to the increase of the volumetric fraction of chrome carbide and of the volumetric fraction of chrome oxide because these stages have smaller densities in relation with the metal phase. The maximal speed corresponding to the point 3 [11] position is that of the going out from the spraying pistol.

A very important data for the high- speed projection system is the projection speed  $v_p$  to the recommended projection distance  $L_s = z - L$  [11], in this case  $L_s = 0,3\text{ m}$  from the evacuation orifice of the high-speed flame spraying pistol.

Also it is important the spraying time of the particle  $t$ . Experimentally there were realized projections for recommended distances between  $0,2\text{ m}$  and  $0,4\text{ m}$ .

The results are in relation with the suffered adhesion by recovering and depend on the mass transfer that may take place during the spraying.

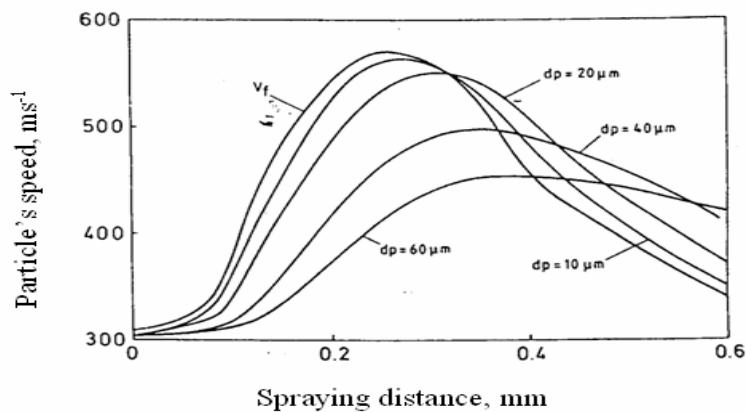


Fig. 1. Variation of the projection speed of the thermal with projection distance spraying particles

Also it is important the spraying time of the particle  $t$ . Experimentally there were realized projections for recommended distances between 0,2 m and 0,4.m.

The results are in relation with the suffered adhesion by recovering and depend on the mass transfer that may take place during the spraying.

The suffered adhesion is essentially proportional to the existent pressure difference between the combustion chamber and exterior. This pressure difference depends on the particle's speed especially on the discharge to the highest density and on the fluid's speed.

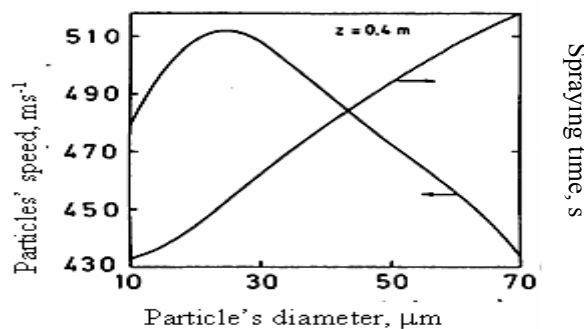


Fig. 2. Variation of the maximal speed of the thermal spraying particle and of the distance spraying time  $z = 0,4 \text{ m}$ , depending on the particle's diameter

In figure (1) it may be observed how the maximum of the fluid and particle's speed obtained as a result of the used mathematical model is met in the interval from 0,2m to 0,3m.

The spraying time increases with the particle's diameter. The particle's speed  $v_p$  increases with the increase of the final volumetric chrome carbide fraction (fig.3).

This speed increases with the final volumetric chrome oxide fraction. Both tendencies take place as a result of the fact that the oxide and the chrome carbide have a bigger density than nickel Ni and chrome Cr in metal phase.

The thermal spraying time of the particle decreases during the increase of the volumetric chrome carbide fraction  $\varepsilon$  and the initial volumetric chrome carbide fraction  $\varepsilon_0$  (fig. 4).

In the figure (2) shows how the speed  $v_p$  initially increases as a result of the fluid acceleration reaching the maximum value when  $d_p = 10 \mu\text{m}$  and decreases then as a result of the particle dimension increase.

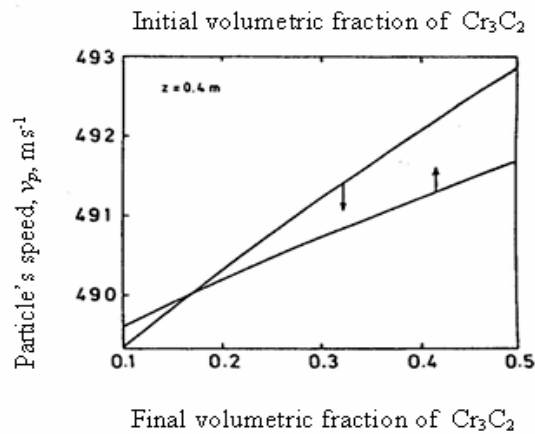


**Fig. 3.** Variation of the particle's speed at  $z = 0,4\text{m}$  depending on the initial and final volumetric fractions of chrome carbide  $\text{Cr}_3\text{C}_2$

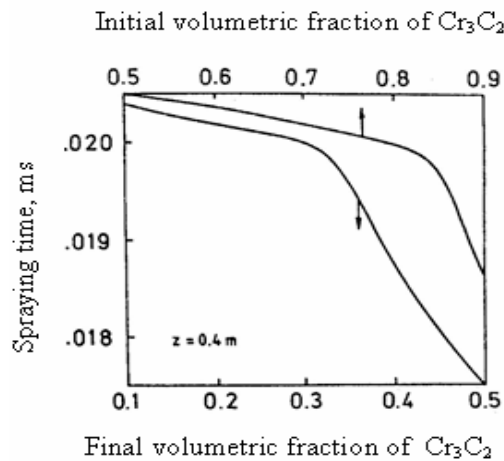


**Fig. 4.** Variation of the thermal spraying particle time depending on the initial and final volumetric fractions of  $\text{Cr}_3\text{C}_2$

**The particle thermal behavior. Comparison with the results experimentally obtained.** Because of the heat and materials scattering coefficients that constitute bigger particles (without taking into account the chrome oxide which is present in a small quantity), the temperature variation inside the particle is little. That is why it is considered only the temperature from the particle surface.

As it may be observed in the figure (5), during the high-speed flame spraying process the powder particles reach the fusion temperature of the Ni Cr metal phase. During the fusion, the particle's temperature increases slowly as a result of the fusion latent heat absorption. After this fusion, the particle's temperature  $T_p$  increases rapidly reaching its maximal value  $T_{p,max}$ . When it is reached the liquid's temperature from the metal phase it starts the solidification and the particle's temperature decreases slowly, this significant decrease of the fluid's temperature having place as a result of the latent heat loss. The heating of the particles with big diameter is relatively small. At the increase of the particle diameter the maximum temperature of the particles  $T_{p,s}$  goes to the sub-layer surface.

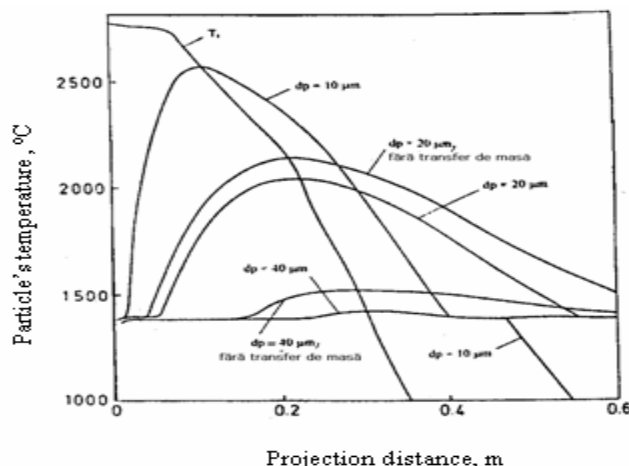


Fig. 5. Variation of the particle superficial temperature depending on the projection distance

If it is not taken into consideration the carbide decomposition process, the thermal diffusivity of the particles is bigger than in contrary case and that is why the particle reaches a higher temperature. Also, the carbides and oxides proportions have a big influence in recovering as it may be observed in the figure (6); at the increase of the carbides' initial content,  $\epsilon_0$  – the initial volumetric chrome carbide fraction, the particle's temperature increases and determines an increase of the particle's thermal diffusivity.

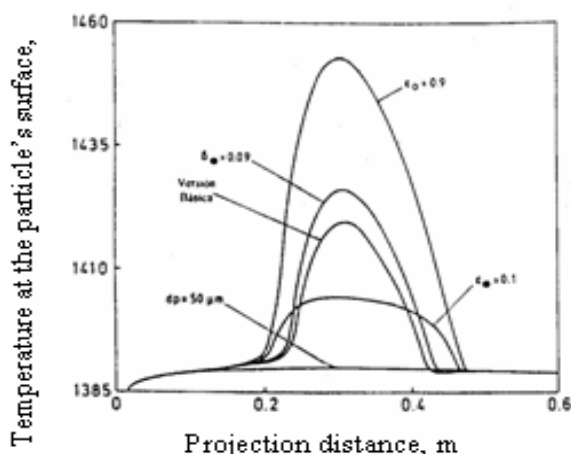
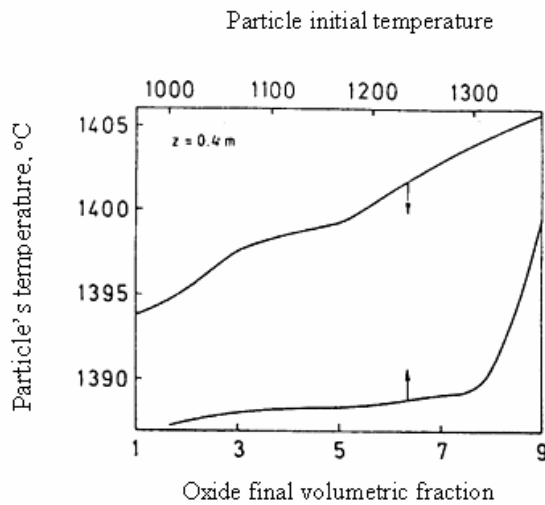


Fig. 6. Influence of the mass transfer process on the particle superficial temperature depending on the projection distance

It is more complete the situation when the final volumetric carbide fraction  $\epsilon$  decreases. On the other hand, the decrease of  $\epsilon$  supposes an increase of the decomposition suffered by the carbides and that involves a decrease of the particles' thermal diffusivity and an increase of the temperature. Also, it involves a decrease of the particle's speed as a result of the density increases that leading to the size of the stationary time where the fluid's temperature is high. On the other hand, the decrease of the particle's speed provokes at its turn a decrease of the heat transfer coefficient  $\alpha$  between the particle's surface and the fluid.

The competence between these two factors will provoke the behavior of the particle's temperature when the  $\epsilon$  carbide final volumetric fraction decreases. First, the particle's temperature is superior to that whose it corresponds the basic situation, when  $\epsilon = 0,3$ . Then, it appears the situation contrary to the initial one, of cooling before solidification in the final moments.



**Fig. 7.** Variation of the particle's temperature at  $z = 0,4\text{m}$  depending on the final volumetric fraction of  $\text{Cr}_3\text{C}_2$

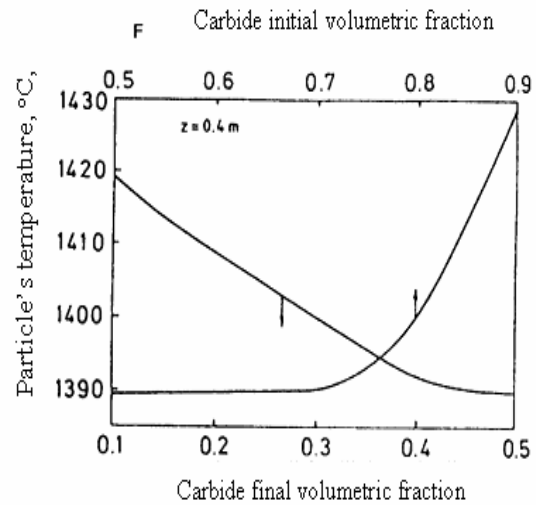


**Fig. 8.** Variation of the particle's temperature at  $z = 0,4\text{m}$  depending on the initial and final volumetric fractions of  $\text{Cr}_3\text{C}$

The increase of the chrome oxide final volumetric fraction  $\delta$  leads to the decrease of the particles thermal diffusivity and of their density. This involves an increase of the particles' speed and the increase of the heat transfer coefficient  $\alpha$ . When this factor is prevailing, the temperature of the particle increases.

This situation is presented in the figure (7). The temperature of the particles with big diameter,  $d_p = 350\mu\text{m}$ , varies slowly. As equal as the mechanical behavior, for the high-speed flame projection process is the knowledge of the temperature maximal values  $T_{p, \max}$  and the longitudinal co-ordinate  $z_m$  where the particle arrives and also the temperature that a particle has to this projection distance.

In the thermal sprayings experimentally realized at distances  $z = 0,2\text{m}$ ,  $z = 0,3\text{m}$  and  $z=0,4\text{m}$  there are not observed significant differences between the decomposing thermal processes. In the figures (5) and (6) it is presented the way in which the maximal temperature  $T_{p, \max}$  for the particles with diameters between  $20\mu\text{m}$  and  $40\mu\text{m}$  depends on the projection distance that is approximately from  $0,2\text{m}$  to  $0,3\text{m}$  from the out going of the spraying pistol. The superheating of the little particles that justifies an increase of the porosity for smaller projection distances without taking into account the main factor of the porosity's increase constitutes the decrease of the particles' speed, the decrease of the particles' kinetic energy. This effect is strictly related to the increase of the spraying distance.

The temperature value  $T_{p, \max}$  increases with the initial temperature of the particle  $T_{p0}$  with the chrome carbide initial volumetric fraction  $\epsilon_0$  and with the chrome oxide final volumetric fraction  $\delta$ . The maximal temperature of the particle decreases when the chrome carbide volumetric fraction increases. The parameter  $z^*$  decreases in the same time when the chrome oxide final volumetric fraction  $\delta$  does, it increases with the particle's initial temperature  $T_{p0}$  and  $\epsilon^*$  behaves un-uniformly with the chrome carbide volumetric fraction  $\epsilon_0$  reaching its maximal value when  $\epsilon_0 \sim 0,82$ .

The figures (8) show how the temperature  $T_{p^*}$  at a projection distance of  $0,3\text{ m}$  from the out going of the spraying pistol increases with the parameters  $T_{p0}$ ,  $\delta$ ,  $\epsilon_0$  and decreases with  $\epsilon^*$ .

From the experimental point of view, the variation  $T_{p^*}$  that depends on the particles' diameter  $d_p$  is very important and it may be observed how the temperature  $T_{p^*}$  decreases when the chrome

carbide dissolution takes place and when the projection distance increases. For the experimental results already described it seems obvious that the projection conditions are better when the spraying distance decreases considering the thermal point of view when the difference between the temperatures  $T_{p^*}$  that correspond to different diameters of the particles in a particles' dimensions distribution interval is not very stressed there may obtained recovering/better layers, then a better superheating and a better porosity.

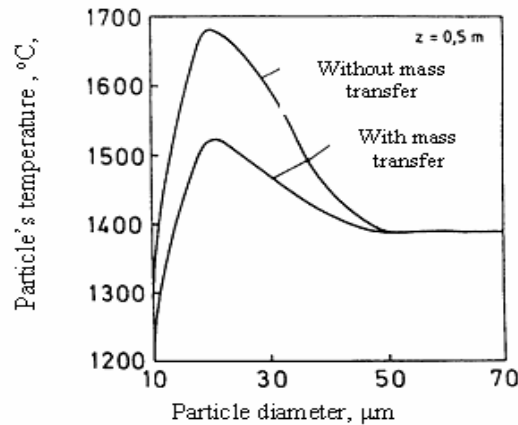


**Fig. 9.** Variation of the particle's temperature depending on its diameter for different positions of the sub-layer at  $z=0,5$ , with or without carbides' transfer

Considering the same figures (9) it may be observed that in the processes of mass transfer between the powder particles it results a difference of much better temperature  $T_{p^*}$  and the interval of the particles' optimal diameters is small.

It results that for any distances there are taken into account the optimal thermal conditions and the distribution of particles' dimensions.

## Conclusions

There was realized a mathematical simulation in order to describe the dynamic processes that take place during the thermal spraying of the powder particles composed of metal matrix and phases with high point to fusion (in this case, the chrome carbide). In the respective model there are taken into consideration the combustion processes, the particles' dynamic and the fluid (inside and outside the spraying jet) and also the mass and heat transfer processes.

At the increase of the chrome carbide and chrome oxide volumetric fraction, the maximal speeds that particles reach and the position in which these speeds are obtained go to the outgoing of the thermal spraying pistol (point 3, figure 1).

The speed of the particles at recommended projection distance ( $L_s = 0,3m$ ) varies depending on the size function and the powder particles diameter. First, it increases till the reaching of its maximal value  $v_{max}$  for  $d_p \geq 25\mu m$  and then it decreases. Also, this speed increases when the chrome carbide final volumetric fraction decreases and the chrome oxide final volumetric fraction increases. The particles' spraying time increases with the diameter and decreases with the initial and final chrome carbide volumetric fraction.

The particle's temperature increases reaching its maximal value and decreases with the size of the spraying/projection distance. During the metal phase fusion and solidification the temperature varies slowly as a result of latent heat absorption and desorption. The carbide decomposition causes the decrease of the particle's temperature.

The particle's temperature increases with the chrome carbide initial volumetric fraction and chrome oxide final volumetric fraction. The decrease of the chrome carbide final volumetric fraction leads to the decrease of the particle's temperature in the total fusion region while in the anterior and posterior regions it increases.

The maximal temperature of the particle increases with the initial particle temperature, with the chrome carbide initial volumetric fraction and with the chrome oxide final volumetric one. This maximal temperature decreases when the chrome carbide final volumetric fraction increases. The chrome carbide final volumetric maximal position increases with the initial temperature of the particle and with the chrome oxide final volumetric fraction.

The particle's temperature at the distance where the sub-layer ( $L_s = 0,3m$ ) increases with the initial temperature of the particle, with the chrome carbide initial volumetric fraction and the chrome oxide final volumetric one and decreases with the chrome carbide final volumetric fraction. If the thermal spraying distance modifies from  $L_s = 0,3m$  to  $L_s = 0,4m$ , the particle's temperature decreases.

## References

1. Sobolev V.V., Guilemanz J.M. s.a., *Surf. Coat. Technology*, vol.64, pg. 181-187.
2. Parkery D.W., Kutner G.L., *Advise Mater. Proces*, pg. 7, 31-35, 1994.
3. Sobolev V.V., Guilemanz J.M. s.a., University of Barcelona, Barcelona, *Comunicacion Privada*, Surf. Coat. Technology, 1996.
4. *Introduction to the CDS Technology, Plasma Technique AG*, Wohlen, 1990, pg.12.
5. Guilemany J.M., Calero J.A., University of Barcelona, Barcelona, *Communication Privada*, 1995.
6. Han K.S., Chung M.K., Sung H.J., *Transfer ASME, Journal Fluid Engineering*, vol. 113, pg.130-136, 1991.
7. Sobolev V.V., Guilemanz J.M., Calero J.A., University of Barcelona, Barcelona, *Therm. Spray Technology*, 4(3), pg. 276-287, 1995.
8. Gordon S., McBride B., *NASA, Lewis Research Center*, pg. 273, 1976.
9. Swank W.D., Fincke J.R. s.a., *Thermal Spray Industrial Application*, ASM International, Materials Park, Ohio, pg. 313-318, 1994.
10. Guilemany J.M., Nutting J., Lorca-Isern N., *Powder Metallurgy*, vol. 37(4), pg.6-16, 1994.
11. Petrescu D., Antonescu N.N., Neacșu M., *The modulation of the dynamic processes at the thermal spraying with high-speed flame Buletinul nr. 3. LVIII, Seria tehnică, Universității Petrol-Gaze din Ploiești, Ploiesti*, 2006.

## Simularea procesului dinamic de pulverizare termică cu particule de pulbere $Cr_3C_2-NiCr$ și flacără de mare viteză

### Rezumat

În lucrare se prezintă problema termică și cea mecanică a particulei din procesele dinamice la pulverizarea termică cu flacără de mare viteză. Această problemă de dinamică a fluidului s-a realizat teoretic cu ajutorul algoritmilor descriși în lucrarea[11] și experimental în laboratoarele Centrului de Proiecție Termică la Universitatea din Barcelona. Depunerile au fost făcute pe substrat de  $34Cr4Mo$ , de la distanțe diferite de pulverizare ( 200 mm, 300 mm, 400 mm).